Uncertainty analysis related to Beach Morphology and Storm Duration for more Reliable Early Warning Systems for Coastal Hazards.

J. L. Garzon[1†], T. A. Plomaritis[2] and O. Ferreira[1]

[1]CIMA – Centre for Marine and Environmental Research, FCT, Universidade do Algarve, Campus de Gambelas, 8005-139 Faro, Portugal.
[2]Faculty of Marine and Environmental Science, Department of Applied Physics, University of Cadiz, Campus Rio San Pedro (CASEM), Puerto Real 11510, Cadiz, Spain.

†Corresponding author: Juan L. Garzon (jlhervas@ualg.pt)

Key Points:

- Initial morphology governs the eroded volume and controls the final berm width for moderate events and dune retreat for energetic events.
- Storm duration has a limited effect on berm erosion but it can determine the occurrence of dune breaching for very energetic events.
- Early warning systems must consider the variability of the initial beach morphology and storm duration for more reliable predictions.

Abstract

Early warning systems (EWSs) for coastal erosion are highly cost-effective instruments for disaster risk reduction. Among other aspects, an adequate pre-storm beach morphology and the storm characteristic definition are relevant in determining EWSs prediction reliability. Here, XBeach simulations were used to investigate the beach-dune response to different storm events with varying duration and pre-storm morphologies. Severity was defined using wave height return periods (from 5 to 50 years) and duration variability was established by confidence intervals after an adjustment with wave height. Beach morphology variability included different berm morphologies, including erosional and accretional conditions. Three erosion indicators were used: remaining berm width, dune retreat, and eroded volume. Regarding the pre-storm morphology variability: i) pre-storm conditions highly determined the final berm width for the 5- and 10-year events; ii) antecedent morphology affected dune retreat variability mostly for the 50-year events, and; iii) eroded volume depended on the pre-storm conditions, but the percentage of the eroded volume, relative to the initial conditions, was similar regardless of the morphology. Regarding the storm duration effect: i) this variable had a limited impact on the remaining berm width for the 5-year event; ii) storm duration influenced dune retreat mainly for the 50-year event, determining dune breaching occurrence, and; iii) eroded volume response to changes in duration was similar regardless of storm intensity, except for the 50-year event. According to the obtained results, the implementation of reliable EWSs for coastal erosion needs to assess the uncertainties related to initial/forcing conditions, namely pre-storm morphology and storm duration.

Plain Language Summary

Large sea storms generate high waves that can erode or remove sand from the coast, damaging recreational infrastructures and even building foundations. Under these dramatic situations, early warning systems (EWSs) are helpful instruments to alert communities about the risks of the incoming storms. EWSs normally use computational models to calculate sand removal based on the shape of the beach before the arrival of the storm (so-called pre-storm profile) and storm characteristics. The pre-storm profile is not fixed but evolves along the year as the response to the incoming waves. However, updated measurements of the pre-storm profile are not always available. Regarding the storm characteristics affecting coastal erosion, we investigated the importance of the period of time in which high waves are reaching the beach (so-called storm duration). The computational model results display that the pre-storm profile used by this model must be close to reality to obtain reliable predictions of the beach and dune erosion. While less impactful to produce accurate beach and dune change predictions, storm duration should be also considered in the model. This research highlights the importance of knowing the pre-storm profile and storm duration to develop EWSs providing reliable predictions to reduce damages in coastal communities.

1 Introduction

Many coastal zones are heavily populated and host highly relevant socioeconomic activities (e.g. recreation and tourism). Among the different coastline typologies, sandy beaches and dunes occupy 30% of the global coastline (Luijendijk et al., 2018). These features represent the interface between land and ocean and protect many coastal communities against flooding and erosion. However, an important portion of these sandy environments is currently suffering from

long-term structural erosion or landward shoreline migration (Mentaschi et al., 2018). On a shorter temporal scale, beaches can be subject to the impact of severe coastal storms inducing catastrophic morphological changes, exacerbated if the sediment budget is limited, and consequently, compromising the protected urbanized areas. Some examples of the recent storms causing devastating erosive episodes are Hurricane Sandy 2012 (Smallegan et al., 2016), Storm Hercules 2014 (Castelle et al., 2015), Storm June 2016 (Harley et al., 2017), Storm Emma 2018 (Ferreira et al., 2019), or Storm Gloria 2020 (Amores et al., 2020). Moreover, beach erosion will be enhanced in a climate change scenario, with rising sea levels and changes in storminess (Ranasinghe, 2016; Vousdoukas et al., 2020).

Under this threat, the implementation of effective disaster risk reduction (DRR) plans is vital for minimizing damages in occupied areas (Lavell et al., 2012). A key aspect in the effectiveness of the DRR measures is community preparedness allowing, for example, timely site evacuation or effective intervention prior to the approaching storm. In this regard, early warning systems (EWSs) play an important role by combining timely and accurate hazard predictions with the associated risk levels for specific coastal receptors (Harley et al., 2016a; Lavell et al., 2012). The successful implementation of EWSs is one of the most cost-effective and efficient measures for disaster risk reduction and the saving of lives (Ciavola et al., 2014). However, these systems do not form part of many integrated strategies for coastal risk reduction, and specifically warning systems dealing with storm-induced erosion hazards.

Two types of modeling approaches have been implemented in operational and early warning systems to predict beach-dune profile changes: descriptive conceptual models (e.g. Sallenger, 2000) and process-based models (e.g. Roelvink et al., 2009) - authors are not aware of the integration of the equilibrium profile theory-based models such as the convolution model developed by Kriebel & Dean (1993) in EWSs. For instance, the 'Total Water Level and Coastal Change Forecast Viewer' managed by the US Geological Survey, predicts the timing and magnitude of water levels at the shoreline and the potential impacts to coastal dunes. The empirical wave runup parameterization given by Stockdon et al. (2006) provides inputs for the storm impact scale model proposed by Sallenger (2000), which determines the coastal response. This efficient forecast system covers coastal regions from the entire US East Coast and certain areas of the Gulf of Mexico. A similar approach was implemented in an EWS developed in the French Aquitaine Coast resulting in general information of the most exposed coastal sectors at the regional scale and impact intensity at a smaller scale (Lerma et al., 2018). While this is a rapid and simple method of determining the likely effects of storms on dune systems, if a more accurate and detailed-scale prediction of the storm impacts is required, more complex models and coastal information should be considered.

Regarding the process-based modeling approach for the development of an EWS, a few studies are found in the literature (Barnard et al., 2014; Harley et al., 2016a; Plomaritis et al., 2018; Poelhekke et al., 2016; Seok & Suh, 2018; Valchev et al., 2014, 2016; Vousdoukas et al., 2012b). In all these systems, the coastal erosion component is operated by XBeach, a depth-averaged (2DH) morphodynamical model solving cross-shore and alongshore equations for wave propagation, flow, sediment transport, and bed-level changes (Roelvink et al., 2009). Infragravity wave motions and the related wave bore eroding the dune face during storm events are simulated as well (Roelvink et al., 2009). This process-based model is more flexible, robust, and complex than conceptual models; however, it necessitates more data for model setup, must be calibrated, and is widely more time-consuming. The latter aspect might represent a major limitation for

operational systems as the computational time of the online simulations is limited to the short period between the release of successive meteo-marine forecasts (Poelhekke et al., 2016). In order to overcome this limitation, some of the previously mentioned EWSs are based on a system trained with pre-computed or offline process-based model simulations (e.g. Poelhekke et al., 2016). The main advantage of these systems is that the computational time is not limited within that short period and still preserves the capabilities and robustness of a process-based model. Then, for forecast purposes, the offline simulations-based EWSs can be conditioned with wave-surge operational systems to predict instantaneously coastal storm impacts.

These characteristics make this approach suitable for a real-time prediction system (Van Dongeren et al., 2014). Nevertheless, the pre-computed or offline simulation procedure has some limitations. Firstly, for operational purposes, the fundamental variables describing a storm event must be known beforehand to condition the offline simulations-based EWS. While storm duration can span from few hours to more than one week (Arnoux et al., 2021; Castelle et al., 2015; Ferreira et al., 2019; Mendoza et al., 2011), depending on the synoptic history of the storm, many oceanographic prediction systems that can be used to condition those EWSs only deliver forecasts for 72 hours. Hence, the prediction systems might capture the peak of the storm, but the duration of some severe storms might not be available, increasing the uncertainty of the predicted erosion. In fact, as Kriebel & Dean (1993) demonstrated with their time-dependent beach profile model, shorter storms having the same wave height peak result in less beach erosion. In line with that study, several authors (Beuzen et al., 2019; Callaghan et al., 2008; Poelhekke et al., 2016; Santos et al., 2019; Sanuy et al., 2018) included storm duration among the variables when creating the training dataset for estimating coastal erosion. Secondly, pre-computed simulations cannot incorporate changes in the topography/bathymetry profile (only by adding new training data). While this limitation would only apply to the offline approach, in reality, most of the online operational simulations are performed by using a static initial topo-bathymetry due to the difficulties and costs of continuously updating sea bottom information (Harley et al., 2016a) and the subsequent integration of this information into the models. The pre-storm or antecedent profile can also determine the response of a beach-dune system to coastal storms (Beuzen et al., 2019; Crapoulet et al., 2017; Splinter et al., 2018), and consequently, damages in developed areas. Ferreira et al. (2019) demonstrated that a wide berm contributed to minimizing erosion-induced risks for a severe storm in a barrier island system. Moreover, differences in the modeled initial profile can be relevant when the beach is impacted by a storm clustering and full recovery is not possible within the storm sequence.

In this study, the relevance of these two limitations of the EWSs (previously unknown storm duration and static initial beach morphology) will be investigated. The variability of the coastal erosion induced by different storm durations will be quantified along with the system response sensitivity to the pre-storm beach morphology. This research aims to evaluate the coastal erosion uncertainty related to these variables, and ultimately, contributing to building more reliable EWSs. To achieve this objective, a new methodology will be developed that will enable the assessment of the importance of different variables in an EWS. The numerical experiments were designed based on hydrodynamic data and topo-bathymetry information collected in Praia de Faro, southern coast of Portugal (Figure 1 a), selected as a demonstration site for this study.

2 Materials and Methods

2.1 Study area

This numerical study was conducted in Praia de Faro, an open sandy beach located in the Ancão Peninsula (Figure 1 b-c), in the western flank of the Ria Formosa barrier island system. The area presents a steep and narrow beach-face with a single or double berm, depending on the storm intensity and recovery conditions, that range from 15 m to 40 m (Ferreira et al., 2016; Martins et al., 1996). The depth of closure is approximately 10 m below mean sea level MSL (Almeida et al., 2011b). The urbanized area is protected with buried rocks/walls or a natural beach/dune system. This dune varies alongshore with higher volume and elevation at the western and eastern sectors of Praia de Faro, while at the central part, the dune is lower and more fragmented. Sediments are medium to very coarse sand with d50~0.5 mm (Vousdoukas et al., 2012b). Astronomical tides are semi-diurnal, with an average range of 2.8 m during spring tides and 1.3 m for neap tides, while the storm surge levels are relatively low (< 1 m) (Almeida et al., 2012). Therefore, tide conditions are more important in influencing the maximum water level than the surge itself (Fortunato et al., 2016). The wave climate has an average annual offshore significant wave height (Hs) of 0.92 m, with the 70% of the waves traveling from W–SW (71%) and the 23% from E–SE (Costa et al., 2001). Due to the cuspate shape of the Ria Formosa, the site is exposed to the W–SW dominant conditions, whereas it is relatively protected from E–SE conditions.

Figure 1. Location map. a) The Iberian Peninsula with the red polygon highlighting the southern coast of Portugal. b) The location of the Ancão Peninsula (red polygon). c) Demonstration site: Praia de Faro. The polygon highlights the location where the topographical measurements described in section 2.3 were taken.

2.2 Synthetic events at Praia de Faro

The sensibility of the beach-dune system response to storm duration and the pre-storm beach morphology was investigated by quantifying the erosion caused by storms with different wave height return periods T_R (<1, 5, 10, 25, and 50 years). The expression presented in Pires (1998) for SW events was used to compute the wave height associated with those return periods (Table 1). The rest of the variables defining the storm such as peak period (Tp), storm duration, and storm surge were estimated by using deterministic formulations derived from data collected in the Faro Buoy, placed at 93 m depth near Praia de Faro, and a 60-km distant tidal gage (Huelva,

Spain). Previous studies have stated the dependence between wave height and those variables for this coastal area (Almeida et al., 2012; Poelhekke et al., 2016; Rodrigues et al., 2012). The data used to build the expression relating wave height and peak period were collected between 1993 and 2019 and includes only W-SW storm events (Hs > 2.5m, according to Almeida et al. 2012) with at least 3 h of duration. Thus, wave height, and the associated peak period data, were clustered in 0.5 m wave height bins. Subsequently, the mode of the values of Hs and Tp within each bin was calculated. Following previous works that found an exponential relation between Hs and Tp (Mangor et al., 2017), a power expression as a function of the wave height was adjusted to the mode data (Figure 2).

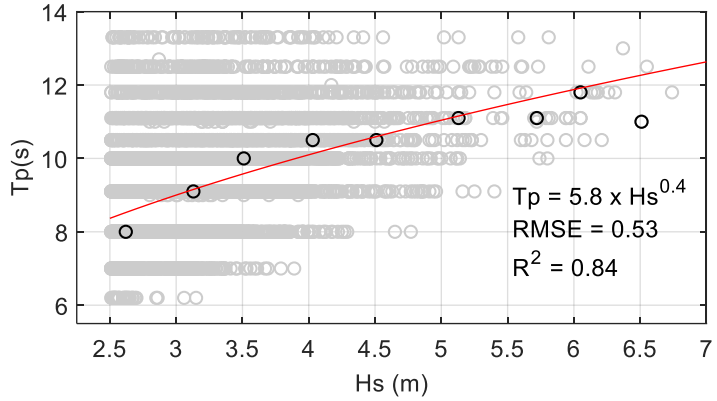

Figure 2. Relationship between Hs and Tp for W-SW storm waves (grey circles) and the statistical skills of the fit (red line) to the mode data (black circles): root-mean-square-error and R-square.

Regarding the estimation of storm duration, Poelhekke et al. (2016) fitted marginal distributions of observations measured at the Faro Buoy, and in combination with copulas describing the Hs-duration pair, generated multiple synthetic pairs of these variables. Copulas are mathematical tools that can be used to construct distributions while preserving the natural variability of the observations (Poelhekke et al., 2016). Following this approach, one hundred synthetic pairs of Hs-duration were generated. The data revealed a strong correlation between these two variables ($R^2 = 0.81$) and a p-value lower than 0.05 denoting a statistical significance (Figure 3). This correlation allowed to obtain a linear relationship that described the storm duration as a function of the wave height. Also, to cover the possible range of storm durations for each specific wave height, the 95% confidence bands were estimated (Figure 3). Thus, for each return period and associated wave height, three storm durations were considered: low (duration 1) and high (duration 3) corresponding to the respective confidence boundaries, and the intermediate (duration 2) from the adjusted fit expression (Table 1).

Total water levels were computed as the combination of astronomical tide and storm surges. For the former, typical spring tide time-series extracted from Plomaritis et al. (2018) were selected while for the latter, the relationship between Hs and surge established by Rodrigues et al. (2012) was used. Peak periods, significant wave heights, and surges are subject to evolution over the course of an event. This unknown evolution in the synthetic events was schematized by a linear increase, until reaching the peak of the storm at half of the storm duration, with the subsequent symmetric decrease of the wave height and the corresponding surge level (Santos et al., 2019).

This is called triangular shape simplification (Duo et al., 2020). The peak period evolution was computed by assuming constant wave steepness (Plomaritis et al., 2018; Poelhekke et al., 2016). A summary of the main variables representing each storm event is displayed in Table 1.

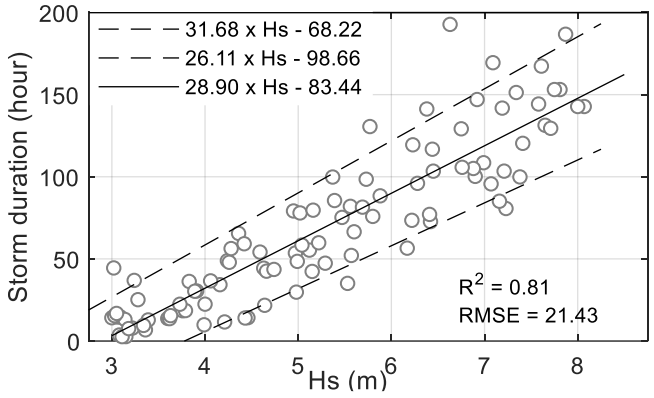

Figure 3. One hundred synthetic events created by the methodology developed in Poelhekke et al. (2016). The solid line represents the linear adjustment between wave height and storm duration and the dashed lines the 95% confidence bounds.

Table 1. Modeled events characteristics

	Return Period (year)				
	< 1	5	10	25	50
Max Hs (m)	3	5.7	6.4	7.4	8.1
Max Tp (s)	9	11.63	12.18	12.91	13.39
Mean direction (deg)	232	232	232	232	232
Max Surge (m)	0.16	0.46	0.54	0.65	0.72
Tide*	Spring tide	Spring tide	Spring tide	Spring tide	Spring tide
Duration 1/2/3 (hour)	-/3/27	50/81/112	68/102/135	95/130/166	113/151/188

*Tide level #3 at Plomaritis et al., 2018. Maximum tidal range 2.42m

2.3 One-dimensional profile definition

Beach topography and bathymetry, oceanic conditions, and sediment sampling have been collected since the 1990s in the study site. Thus, previous authors have classified the site based on the conceptual model of Masselink & Short (1993) as reflective to intermediate (e.g. Almeida, 2007; Ferreira et al., 1997; Haerens, 2009). The beach state at Praia de Faro is highly dependent on the tidal cycle; at high tide, when the beach face is attacked by the waves, the beach is reflective, and during low tide, the beach usually exhibits an intermediate state (Ferreira et al., 1997; Haerens, 2009; Martins et al., 1996). The dominant beach morphologies are mainly Low Tide Terrace + Rip (LTT) and Longshore Bar Trough (LBT), as defined by Masselink & Short (1993) associated with changes in the energy conditions (Almeida, 2007; Ferreira et al., 1997; Haerens, 2009; Martins et al., 1996). The LTT profile is the predominant profile but the type of

the profile depends on the combination of the pre- and post-storm wave conditions, the profile status, and the seasonal variation in the wave climate (Martins et al., 1996). The longshore submerged bar is built under high-energy conditions. Then, under less energetic wave conditions, sediment from the bar is landward transported building a berm or a terrace (Almeida et al., 2011b). If the wave energy is very low, the bar-trough system stays in position, limiting the recovery of the berm or terrace as observed by Almeida (2007) and Haerens (2009). Therefore, sediment lost from the beach face is gained by the sub-tidal terrace, and vice-versa, depending on wave energy (Almeida et al., 2011b). Both the LTT and the LBT features are situated below -1m MSL (Haerens, 2009).

The emerged profile at the site is characterized by the presence of well-developed beach cusps which induce some variability to the beach profile (Balouin et al., 2000; Vousdoukas, 2012a). The beach recovery response is very active after high energy events, with the rapid creation of berms or the widening of the existing ones (Malvarez et al., 2021; Sá-Pires et al., 2006). The average beach face slope (tan β) observed by various authors varies between 0.11 (Ferreira et al., 1998) and 0.14 (Ciavola et al., 1997). Moreover, differences in beach face slope between seasons are less than 0.08 (Haerens, 2009). The slope of the low terrace can range from 0.06 (Martins et al., 1997) to 0.03 (Almeida, 2007). The latter work found that the slope of the longshore bar trough is about 0.02. Also, pre- and post-storm profiles tend to rotate around a point situated between +0.5m MSL and -0.5m MSL (Anfuso & Ruiz, 2004; Sá-Pires et al., 2006). Some portions of the dune line can remain stable at least for events of a 15-year return period (Ferreira et al., 2019; Garzon et al., 2021a).

To model the system response sensibility to beach morphology, different profiles were designed exhibiting the main features described above. That was further supported by the information collected during a monitoring period between 2018 and 2019 that evidences the historically observed natural beach variability of this site (Figure 4). Post-storm conditions (March 2018) were not considered to define the initial (pre-storm) profiles. Details on the monitoring program can be found at Ferreira et al. (2019), Garzon et al. (2020), and Malvarez et al. (2021).

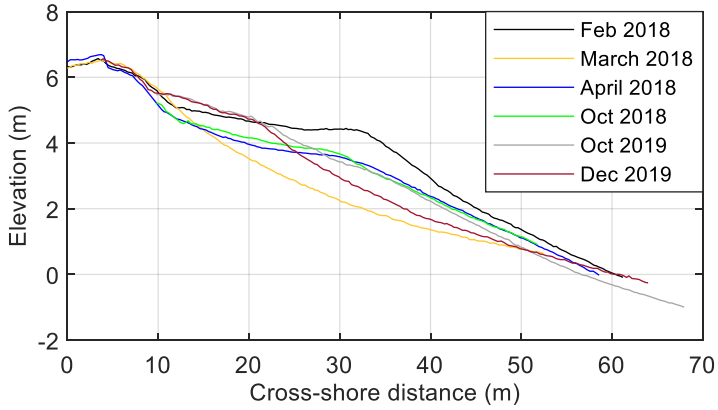

Figure 4. Example of topographical measurements referred to MSL, conducted in Praia de Faro between February 2018 and December 2019.

Four profiles illustrating different emerged beach morphologies were implemented in the numerical model: full high berm, eroded high berm, full low berm, and eroded low berm (Table

2; Figure 5). The submerged part of the profiles was characterized by alongshore bar and a trough (LBT) as reported in the literature and also observed in the 2018 bathymetric survey conducted within the COSMO program (PROGRAMA COSMO, n.d.). Additionally, two other profiles were evaluated, whose emerged parts represented a full high and low high berm profile, and the submerged part corresponded to a Low Tide Terrace (Figure 5).

Table 2. Sand volume (m3/m) measured between 3680 m (MSL) and 3740 m (dune), beach face slope, dune toe elevation (m), and berm characteristics (m).

	Full high berm	Eroded high berm	Full low berm	Eroded low berm
Subaerial volume	223.3	190.0	197.8	182.9
Beach face slope	0.16	0.12	0.12	0.11
Dune toe elevation	5.0	5.0	4.5	4.5
Berm width	20	10	16	12
Berm edge height	4.4	4.7	3.6	3.6

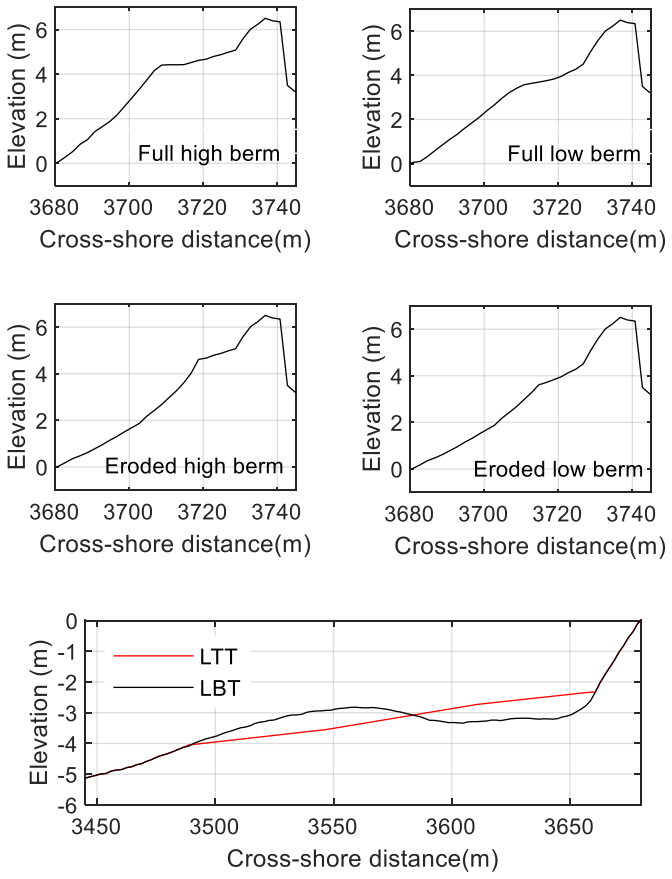

Figure 5. Morphology of the simulated profiles.

2.4 Numerical model framework validation

A multi-model framework, SWAN (Booij et al., 1999) coupled with XBeach (surfbeat), was used to propagate the wave conditions from offshore to the shore and simulate morphological changes in the beach and dune system (see Garzon et al. [2021b] for details). The 1D XBeach grid had a variable cross-shore resolution with a minimum node spacing of 2 m in the surfzone and emerged profile. Model parameters largely impacting the erosion of the steep profiles such as 'facua', and 'wetslope' (Cho et al., 2019; Garzon et al., 2021b; Simmons et al., 2019; Vousdoukas et al., 2012b) were set to 0.15 and 0.45 respectively. Moreover 'bermslope' was activated and set to 0.12. This is a numerical artifact that creates an onshore sediment transport suitable to simulate erosion in intermediate and reflective sandy beaches (Garzon et al., 2021b; Roelvink et al., 2019). These three parameters were used to calibrate a similar model for the study area in Garzon et al. (2021b). The breaker index, 'gamma' (Roelvink et al., 2009) was set to 0.545. This multi-model approach was validated for the erosion caused by storm Emma (Ferreira et al., 2019) as pre- and post-storm profile measurements were available (Figure 6). The evaluation metrics namely, Brier Skill Score (BSS), root-mean-square-error (RMSE), and bias were 0.96, 0.21, and -0.03 respectively, indicating an excellent model performance.

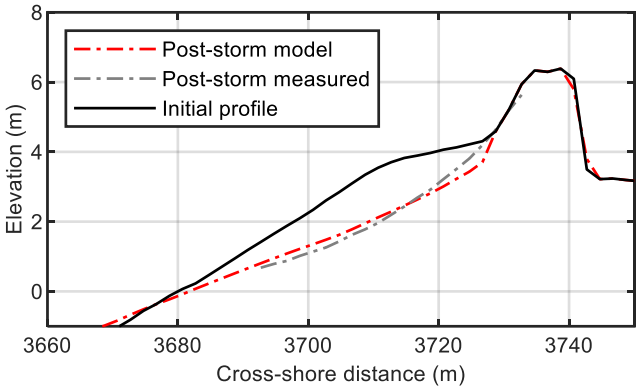

Figure 6. Initial, measured and simulated profiles used for model validation.

2.5 Erosion indicators

Three erosion indicators that are relevant for coastal erosion warning systems, in line with those presented by Ferreira et al. (2017), were included in the analysis: 1) eroded volume of the subaerial region, in absolute and relative terms, computed from MSL (3680 m from origin) to the backside of the dune system (3740 m); 2) dune retreat, estimated as the horizontal profile retreat at the elevation of the dune toe (pre-storm conditions), and 3) remaining berm, measured as the distance between the post-storm berm edge and the dune toe. The sensibility of these indicators to changes in storm duration and the natural variability of the pre-storm morphology was investigated. In addition, using the maximum modeled water levels, for the different tested return periods, and the initial dune/beach morphology, the mechanisms governing dune and berm evolution were analyzed by applying the storm impact regime developed by Sallenger (2000).

3 Results

3.1 Sensitivity to beach morphology

The sensitivity to the pre-storm beach morphologies (Figure 5) was evaluated by analyzing the post-storm profiles simulated using events with duration 2 (see Table 1). For the 5-year event, a 2 m-scarp defining a clear berm was created in those profiles displaying a high berm (Figure 7). Also, the post-storm berm remained wider for the case of the full high berm profiles (LBT) as displayed in Figure 7 and LTT profiles (Table 3). Conversely, the berm was fully depleted after this event on the profiles exhibiting lower berm height (Table 3). For the 10-year event, only the full high berm profiles (LBT and LTT) maintained a short berm after the storm (Figure 7 and Table 3). In the eroded high berm profile, the berm was fully depleted after the event, but the erosion did not reach the dune. On the contrary, dune retreat (1-2 m) was observed in the low berm profiles, with a slightly higher retreat in the weakest profile (eroded low berm) as displayed in Figure 7 and Table 3.

For the 25-year event, the berm was completely depleted after the storm for all beach morphologies. Also, the post-storm dune position was very similar for all profiles. The modeled dune retreat was approximately 4 m in the full high berm profiles (LBT and LTT), while in the rest of the profiles the retreat reached 7 m (Figure 7 and Table 3). For the 50-year event, the dune was severely eroded, but it was not completed dismantled for any of the morphologies. The dune retreat ranged between 7 and 12 m, with the more robust profiles revealing the lowest retreat. Moreover, no differences were found between the post-storm full low berm and eroded high berm profiles for this event (Figure 7 and Table 3). The effect of the submerged morphology in the berm and dune erosion was not relevant and it can be observed that the LTT and LBT profiles resulted in a similar post-storm profile (Table 3 and Figure A1).

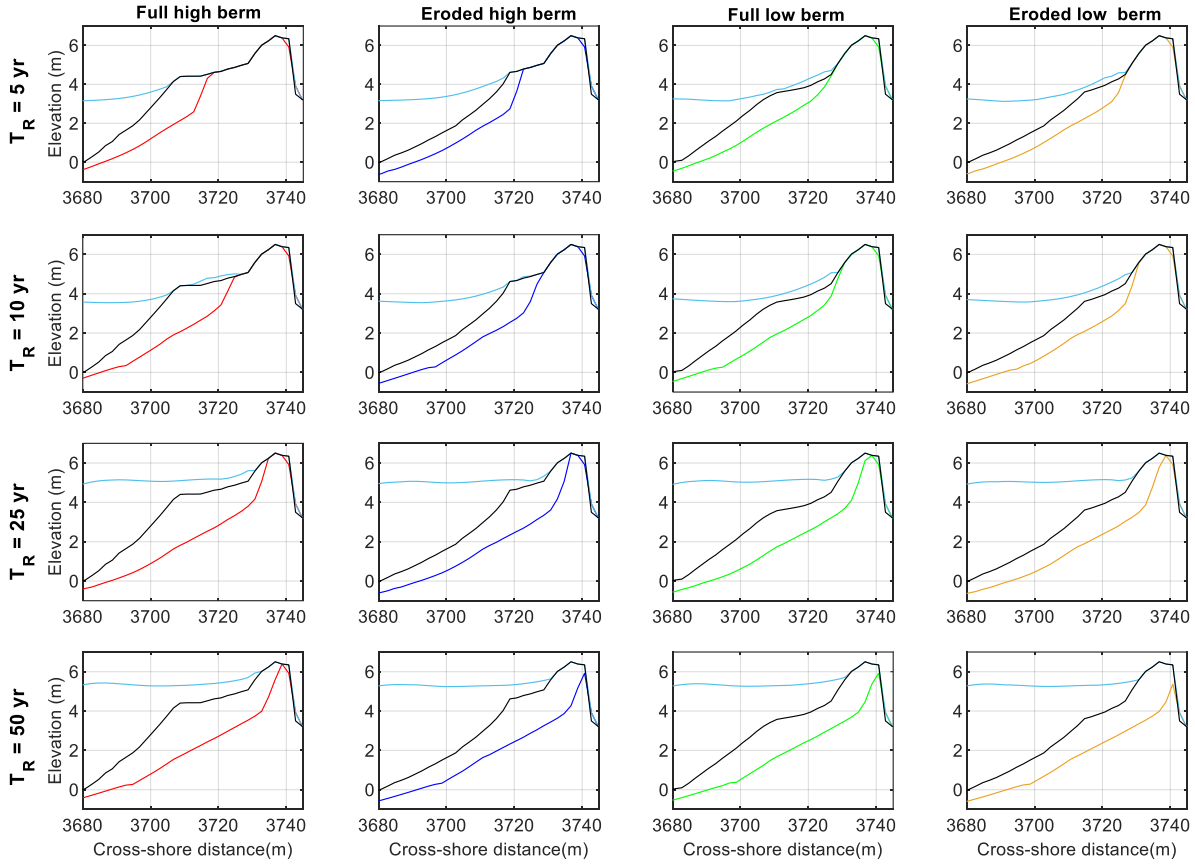

Figure 7. Simulated maximum water level (light blue line), pre-and post-storm LBT profiles (black and colored respectively) for the different events with duration 2. Profiles without a further designation represent LBT morphology.

For the 5 and 10-year events (duration 2), the morphology of the high berm profiles reduced the maximum elevation reached by the sea surface, and the storm impact regime was swash and consequently, the dune was not impacted. (Figure 7 and Table 3). Conversely, the flow propagated further landward in the low berm profiles and the maximum water elevation exceeded the dune toe height (collision regime) during these events (Figure 7). This caused a full depletion of the berm (Figure 7 and Table 3). Thus, different storm impact regimes (swash and collision) were observed depending on the berm elevation for these events, but the collision regime did not necessarily induce always dune retreat (e.g. 5-year event for full and eroded low berm LBT profiles). For the 25-year and 50-year events, the maximum water levels vastly exceeded the dune toe elevation (collision regime) in all beach morphologies causing dune retreat in all of those profiles (Figure 7 and Table 3). A similar regime (collision) was modeled for all profiles under these events, but not discriminating the severity of the dune retreat.

Differences in the absolute eroded sediment (above MSL) were observed as a function of the pre-storm morphology (Table 3). However, the percentage of eroded material was similar for most profiles/conditions, regardless of the initial morphological conditions. For instance, for the 10-year event and duration 2, the sediment eroded was 61.9, 56.0, 52.1 and 51.7 m^3/m for the full high berm, full low berm, eroded high berm, and eroded low berm profiles (LBT) respectively

(Table 3), corresponding to 27-28% of the pre-storm volume for all the beach morphologies (Figure 8). In the case of the 25-year event and duration 2, all beach profiles lost 38-40% of the beach volume above MSL. The most relevant differences were observed in the 50-year event with duration 3, as in some of the profiles the dune was dismantled while in others the back of the dune withstood the storm impact (Figure 8).

Table 3. Change on the erosion indicators for the different tested storm conditions and beach morphologies. Values for simulations with duration 1/duration 2/duration 3, respectively, and the corresponding Sallenger's regime.

	Return Period <1-year			
	Sand volume eroded (m^3/m)	Remaining berm (m)	Dune retreat (m)	Regime
Full high berm LBT	- /2.9/12.6	20/20/20	0/0/0	Swash
Eroded high berm LBT	- /0.7/9.4	10/10/10	0/0/0	Swash
Full low berm LBT	- /1.7/10.7	16/16/16	0/0/0	Swash
Eroded low berm LBT	- /0.7/9.4	12/12/12	0/0/0	Swash
Full high berm LTT	- /2.7/11.6	20/20/20	0/0/0	Swash
Full low berm LTT	- /1.6/10.0	16/16/16	0/0/0	Swash
	Return Period 5-years			
	Sand volume eroded (m^3/m)	Remaining berm (m)	Dune retreat (m)	Regime
Full high berm LBT	36.5/49.1/61.5	12/10/8	0/0/0	Swash
Eroded high berm LBT	28.3/41.2/53.4	6/6/2	0/0/0	Swash
Full low berm LBT	33.3/46.2/ 57.7	Depleted	0/0/1	Collision
Eroded low berm LBT	29.0/42.1 53.6	Depleted	0/0/1	Collision
Full high berm LTT	34.3/44.5/56.1	10/10/8	0/0/0	Swash
Full low berm LTT	31.0/41.7/52.4	Depleted	0/0/0	Collision
	Return Period 10-years			
	Sand volume eroded (m^3/m)	Remaining berm (m)	Dune retreat (m)	Regime
Full high berm LBT	48.7/61.9/72.5	4/4/4	0/0/0	Swash
Eroded high berm LBT	39.1/52.1/63.2	2/Depleted/Depleted	0/0/1	Swash/Collision/Collision
Full low berm LBT	43.0/56.0/67.0	Depleted	1/1/2	Collision
Eroded low berm LBT	39.2/51.7/62.2	Depleted	2/2/3	Collision
Full high berm LTT	46.1/57.1/67.0	2/2/2	0/0/0	Swash
Full low berm LTT	40.1/50.9/60.5	Depleted	1/1/2	Collision
	Return Period 25-years			
	Sand volume eroded (m^3/m)	Remaining berm	Dune retreat (m)	Regime
Full high berm LBT	69.4/86.9/94.1	Depleted	3/4/5	Collision
Eroded high berm LBT	57.7/75.6/83.3	Depleted	5/6/7	Collision

Full low berm LBT	61.6/79.9/86.8	Depleted	5/7/7	Collision
Eroded low berm LBT	56.4/74.6/82.2	Depleted	5/7/9	Collision
Full high berm LTT	63.6/81.2/88.0	Depleted	2/4/4	Collision
Full low berm LTT	56.7/74.0/80.3	Depleted	5/7/7	Collision

Return Period 50-years

	Sand volume eroded (m^3/m)	Remaining berm	Dune retreat (m)	Regime
Full high berm LBT	86.8/99.2/115.8	Depleted	6/7/10	Collision
Eroded high berm LBT	76.4/86.5/116.6	Depleted	8/10/Depleted	Collision/Collision/Overwash
Full low berm LBT	80.4/90.5/120.9	Depleted	9/10/Depleted	Collision/Collision/Overwash
Eroded low berm LBT	75.2/85.2/120.4	Depleted	9/12/Depleted	Collision/Collision/Overwash
Full high berm LTT	84.0/93.6/110.6	Depleted	6/7/9	Collision
Full low berm LTT	75.4/84.6/112.0	Depleted	9/9/Depleted	Collision/Collision/Overwash

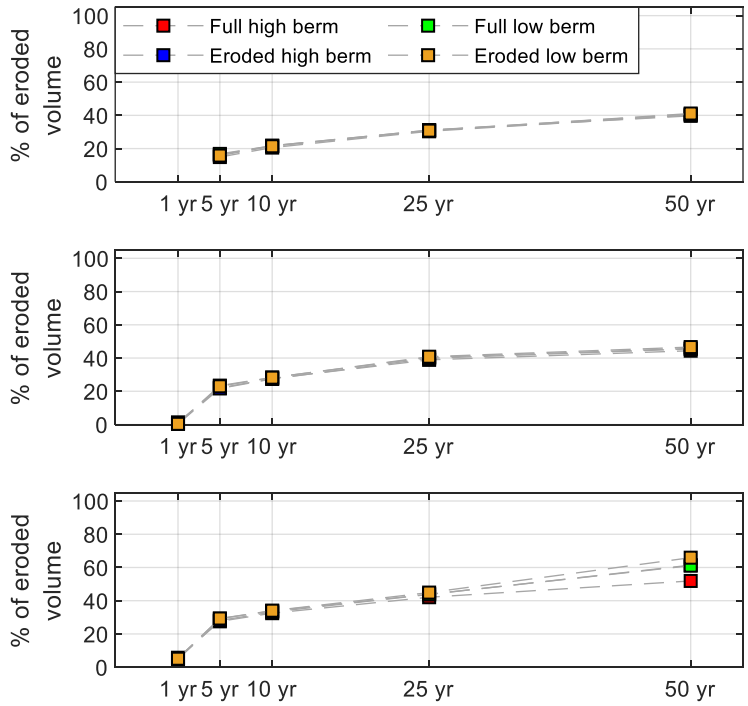

Figure 8. Percentage of material eroded in respect to the pre-storm volume of the subaerial region. The upper panel represents the simulations considering duration 1, the middle is for duration 2, and the lower is for duration 3.

3.2 Sensitivity to storm duration

The storm with the lowest return period did not erode the berm for any of the two durations assessed and for any of the simulated beach morphologies; however, higher sand volume was eroded with the storm lasting for 27 hours (duration 3) as shown in Table 3. For the 5-year event,

differences in berm retreats resulting from the duration 1 and duration 3 simulations were only relevant in the high berm profiles (LBT), reaching up to 4 m (Table 3). In the low berm profiles, all storm durations assessed resulted in berm depletion (Table 3 and Figure 9). The eroded sand volume was slightly more sensitive to storm duration in the LBT profiles, with eroded volume differences between duration 3 and duration 1 about 24-25 m^3/m against 21-22 m^3/m for the LTT profiles. For the 10-year event, both metrics, the remaining berm and dune retreat were barely sensitive to storm duration since simulations with duration 1 and duration 3 revealed similar behavior (Table 3 and Figure 9). Conversely, the eroded volume actively responded to changes in storm duration and differences were around 24-25 m^3/m as well. For the 25-year event, the berm was depleted in all the morphologies for the three assessed durations. Regarding the dune erosion, retreat differences between the simulations with duration 1 and 3 were 2 m, except for the eroded low berm profile where those differences were 4 m (Table 3 and Figure 9). Similar to the other events, the eroded sand volume was very sensitive to storm duration and eroded volume differences between the storms with duration 1 and 3 were 24-25 m^3/m. For the 50-year event, dune retreat was very sensitive to storm duration. In the eroded high berm, full low berm, and eroded low berm profiles, the storm with the longest duration (188 hours) caused dune dismantling while the others with duration 1 and 2 did not. Dune retreat sensitivity to storm duration at the full high berm profiles was 4 m (Table 3 and Figure 9). In those profiles where the dune was dismantled, eroded volume differences between duration 1 and 3 were more significant than in the other less energetic storm events. When comparing the eroded volume sensitivity to storm duration in two highly distant profile morphologies (full high berm and eroded low berm), it can be concluded that the sensitivity to storm duration in both profiles is similar, regardless of the storm severity (except for $T_R = 50$ years), as it is shown in Table 3. Moreover, the dune and berm retreat sensitivity to storm duration was not affected by the submerged morphology, and LBT and STT profiles exhibited a similar sensitivity range (Table 3). For the eroded volume sensitivity, STT profiles obtained slightly lower differences in eroded volume (lower sensitivity) than the LBT profiles (Table 3). The storm impact regime was not very sensitive to storm duration since the peak of the oceanic conditions was identical for the three durations. However, for the 50-year event, while the maximum water levels did not exceed the initial dune crest for any of the durations, the longest storm was capable of lowering the dune crest leading to a shift in the storm impact regime (from collision to overwash). Similarly, the initial dune toe was not exceeded by the maximum water levels for the 10-year event on the eroded high berm morphology, but the total erosion of the berm found for the events with duration 2 and 3 caused the lowering of the due toe leading to a shift from swash to collision regime.

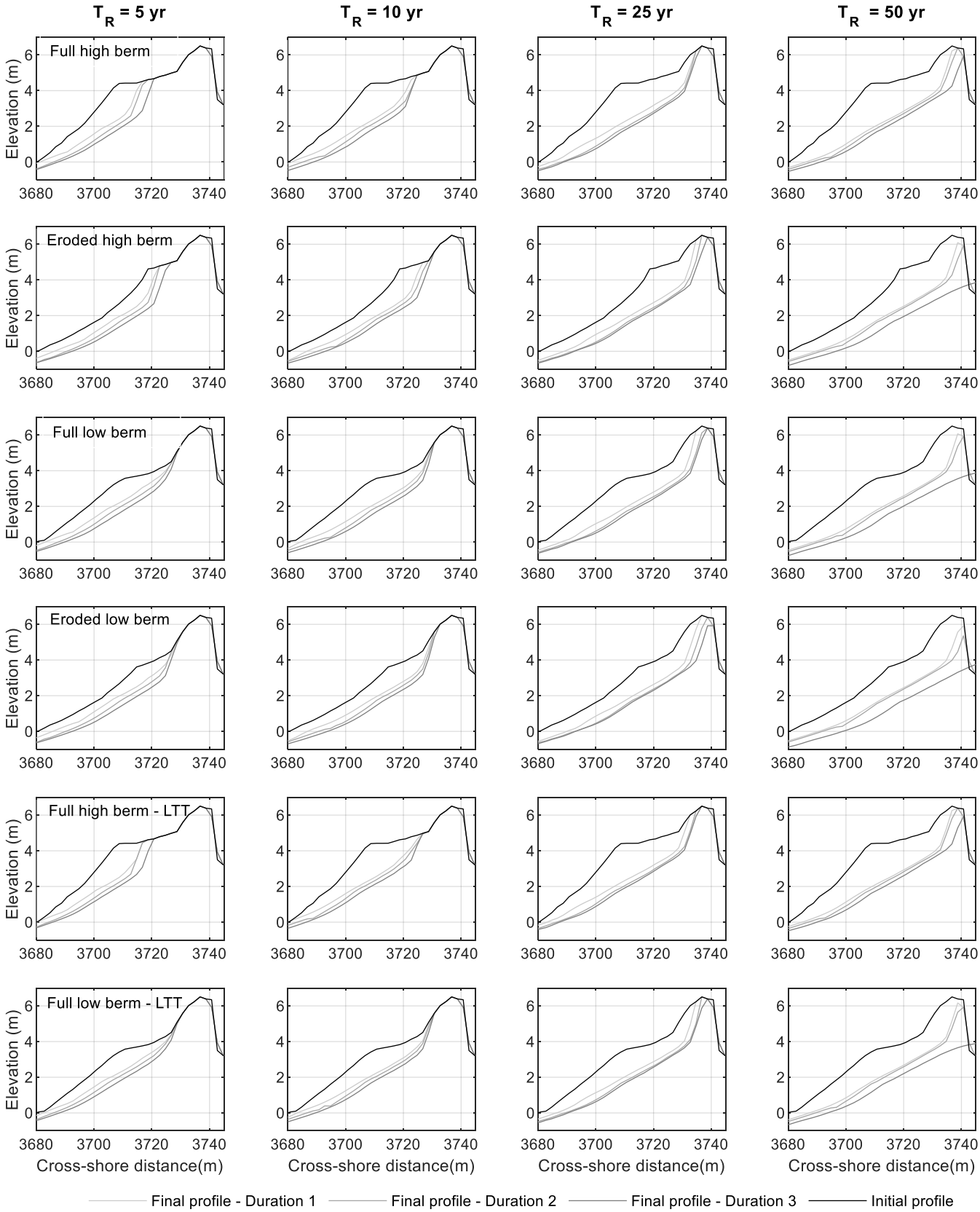
T_R = 5 yr
T_R = 10 yr
T_R = 25 yr
T_R = 50 yr
Full high berm
Eroded high berm
Full low berm
Eroded low berm
Full high berm - LTT
Full low berm - LTT
Elevation (m)
Cross-shore distance(m)
Final profile - Duration 1
Final profile - Duration 2
Final profile - Duration 3
Initial profile

Figure 9. Modeled profiles for different return periods, durations, and initial morphologies. Profiles without a further designation represent LBT morphologies.

4 Discussion

4.1 Model performance

The impact of storms in Praia de Faro has been previously investigated by numerical experiments and field observations. Almeida et al. (2011a) implemented the convolution model (Kriebel & Dean, 1993) along 26 cross-shore profiles to evaluate the vulnerability of this site under the impact of the 25-year event and they obtained minimum, maximum and average dune retreats of 2.5, 15, and 8 m respectively. The dune retreats found in the present experiment were generally lower, for the same return period, ranging between 3 and 9 m. Ferreira et al. (2006) also applied Kriebel and Dean's approach to compute the retreat driven by the 50-year event yielding values of 25 m approximately. This would mean the full dismantling of the dune and eroding a part of the urbanized area. The retreat found in their study exceeded the one computed here (Table 3), where dune depletion was only found for the longest storm (188 hours). A larger retreat provided by the convolution model with respect to the XBeach model was also observed by Plomaritis et al. (2019). The discrepancies between both models can be the consequence of the different approaches to compute coastal erosion: analytical against process-based. While top-down models such as the convolution model are computational efficient (Ferreira et al., 2018; Plomaritis et al., 2019) and thus with a great utility for first assessments, process-based models are more accurate and robust (Callaghan et al., 2013) and should be used for detailed risk assessments, including EWS.

Regarding field observation studies, the impact of the storm Emma, a 16-year return event considering just Hs and more than 20 years if the joint probability between waves and surges is considered (Ferreira et al., 2019), caused dune retreats up to 3 m along the Praia de Faro (Garzon et al., 2021a). Considering that the profile before the arrival of the storm can be classified as a full high berm profile, the observations and the currently used model results agree well.

4.2 Sensitivity to beach morphology

The response of the beach to the 5-year event was conditioned by the berm volume and height. After the formation of the initial beach scarp, the incoming wave energy caused the undercutting of the scarp leading to a scarp toe migration upwards and landwards in all beach morphologies. Then, in the low berm profiles, the lower elevation enabled the maximum water levels to easily exceed the scarp crest during the course of the storm removing this near-vertical feature, similar to the process described by van Bemmelen et al. (2020). Importantly, this occurred before the peak of the storm was reached and the new-formed gentler slope facilitated the inland propagation of the flow, extending the maximum water levels close to the dune toe. As the flow propagated landward, the berm was more intensively eroded. On the other hand, in the high berm profiles, the maximum water levels did not exceed the scarp crest during the storm. Thus, the scarp obstructed the uprush, and the flow did not propagate further inland, limiting the erosion to the seaward side of the scarp. These two different scarp evolutions were also observed by van Bemmelen et al. (2020) who also declared that beach scarps are prone to be formed in high platforms elevations and steep initial beach slopes. Also, according to previous formulations that

relate beach slope and runup (eg., Stockdon et al., 2006), for beaches with uniform slope, one might expect that the full high berm profile simulation revealed the highest total water levels as it had the steepest beach face slope. However, the formation and maintenance of the scarp determined the maximum water elevation. Therefore, while the pre-storm beach morphology determined the berm erosion and the overall regime, the topography did not affect the dune retreat.

For the 10-year event, a scarp was initially created but the maximum water levels rapidly exceeded the scarp crest leading to its removal in all the morphologies. As the storm continued, the berm was progressively eroded. The wider and higher berm of the full high berm profile avoided the total berm depletion, protecting the dune from erosion. Inversely, the low berm profiles represented a lower sand buffer to protect the dune causing dune retreat. As found in previous studies, the berm robustness inversely determined the dune erosion (Beuzen et al., 2019; Crapoulet et al., 2017; Fairley et al., 2020). Moreover, the new-formed gentler slope of the low berm profiles also contributed to farther extend inland the maximum water level, and along with the lower dune toe elevation, allowed the total water levels to exceed the dune toe (collision regime). When waves exceeded the dune toe, the incoming energy collided with the dune resulting in dune erosion. Beuzen et al. (2019) stated that the dune erosion is equally affected by the exceedance of the total water levels above the dune toe and the width of the berm immediately fronting the dune, with wider beaches resulting in reduced dune erosion. For the 10-year event, the pre-storm morphology lost influence in berm erosion and gained some relevance, around 2 m, in dune retreat in comparison with the former event. These 2 m can be considered within the model uncertainties.

For the 25- and 50-year events and all morphologies, the total water levels largely exceeded the dune toe elevation and waves collided with the dune. On these highly energetic events, the dune retreat was mainly controlled by the sand volume with the full high berm profile (150 m3/m) reducing the dune retreat in respect to the rest of the profiles. Also, for the eroded high berm and full low berm profiles, exhibiting similar volume (117 and 115 m^3/m), the final post-storm position was very similar after those very energetic events, while the eroded low berm profile, with the lowest sediment volume (100 m^3/m), was the most eroded one. This demonstrated the importance of the antecedent sand volume (beach face and backshore) in affecting the response of the beach/dune system, in line with other works (Garzon et al., 2021a; Guisado-Pintado & Jackson, 2018). However, if the profiles maintain approximately the same sand volume, even for different morphologies, the post-storm profile is very similar, especially for very high energetic events, as stated by Garzon et al. (2021b). Therefore, when increasing storm severity, the influence of the pre-storm beach morphology, especially the beach volume, raised as well. On the other hand, the LBT and LTT typology did not alter the erosion indicators for any of the events.

In terms of berm volume eroded, profiles with a more robust berm lost more sediment. This was also reported by Harley et al. (2016b), Scott et al. (2016), and Beuzen et al. (2019) who stated that the pre-storm profile was fundamental to determine the berm erosion, with more accreted berms facing larger erosion. However, the percentage of the eroded volume of the subaerial region was not affected by the pre-storm morphology, and for each specific storm, this percentage was very similar across the profiles (Figure 8). This agrees partially with Harley et al. (2016b) observations of berm erosion along a 3500 m coastal stretch after two virtually identical

storms. The authors declared that the beach response, in terms of berm erosion, as the percentage of the pre-storm berm volume, was very similar in these two events. In this study, the percentage of the berm eroded volume (measured from the MSL to the dune toe) varied across the profiles (not shown); however, the percentage of the eroded volume computed in the entire subaerial region (above MSL) of the beach at those profiles was very similar. Moreover, the percentage of eroded volume and wave height return period can be fitted by a power-law expression, as illustrated in Figure 8, similarly to previously suggested by other authors (e.g., Ferreira, 2005; Eichentopf et al., 2019). Likewise, Splinter et al. (2014) used a power-law relationship to represent wave energy density and eroded dry beach volume.

The effect of storm sequences rather than individual storms has been also actively investigated in the literature. Some authors have reported an enhanced beach erosion caused by storm sequences with respect to the impact of individual storms with similar return periods (Baldock et al., 2021; Ferreira, 2005). Assuming an equilibrium-type beach response, beach erosion for a given storm within a cluster depends on the oceanic conditions and the antecedent beach morphology. In this study, the eroded high berm profile would be representative of a post-storm profile after the impact of an approximately 5-year event, while the full high berm morphology can represent a pre-storm profile. Thus, the impact of the 5- and 10-year events in the eroded high berm profile can be considered as a storm cluster formed by 2 storms with the absence of beach recovery. The more eroded berm found after these events in the eroded high berm profile in regards to the full high berm profile (Figure 7) would suggest that storm sequences, within these energy conditions, induced a cumulative effect. When the wave energy highly increases (25-and 50-year events), this pattern was not so evident. Thus, the similar post-storm profiles obtained for all morphologies (it does not necessarily mean the same dune retreat) indicated that an extreme event can generate an almost similar beach profile regardless of storm chronology, as it was stated by Gravois et al. (2016). It is important to remark that the nearshore bar dynamics effect was not considered.

4.3 Sensitivity to storm duration

The effect of the storm duration on the remaining berm and dune retreat indicators was different based on the storm severity and beach morphology. In the 5-year event, the storm duration had an impact on the remaining berm width of the high berm profiles, but not for the other beach morphologies (on these profiles the berm was completely eroded regardless of the duration). On the other hand, the remaining berm and dune retreat were not sensitive to storm duration in the 10-year event for any of the morphologies. In the 25- and 50-year events, the dune retreat response to variability in storm duration was more sensitive. This is especially remarkable for the 50-year event, where the storm duration regulated the dune capacity to endure. Thus, with the longest storm, some of the profiles reached a tipping point in which the dune was dismantled and a possible positive feedback mechanism can be initiated leading to breaching and possible inundation regimes.

The importance of the storm duration on coastal erosion is widely accepted, but previous studies have mainly focused on its effect in eroded volume and less intensively in other coastal erosion indicators such as berm and dune retreat. For instance, based on field observations, Cohn et al. (2019) found an increase in dune eroded volume with increasing storm durations. Similarly, Beuzen et al. (2019) declared that if the dune toe were exposed to the wave action during longer

periods, the dune eroded volume, and dune retreat also increased. Using numerical models, Sánchez-Arcilla et al. (2009) calculated eroded volume variability by estimating the difference between computations for a given height with varying duration. As the present experiment, a linear relationship was adjusted between Hs and duration, and the 95% limits of the corresponding confidence intervals. They found that these differences were higher with higher wave heights. The results presented here displayed another pattern, and the differences in eroded volume resulting from the 5-, 10- and 25-year events with varying storm duration were almost constant. A similar range of durations for all events, ±30 hours (Table 1), can be the reason for this model's response to storm duration. However, other indicators such as dune retreat became more sensitive to storm duration with increasing storm severity.

In the numerical study conducted by Plomaritis et al. (2018) in Praia de Faro (using a full berm profile morphology) the authors concluded that the storm duration did not provide additional information to their probabilistic model and that this variable did not succeed in predicting hazard or no-hazard storm situations. They argued that the copula method used in the study to relate wave height and duration correctly reproduced this association. Also, they found that this approach contributed to limit the number of boundary conditions to be included in their study, highly reducing the training dataset. In the present study, storm duration did not determine the occurrence of dune retreat, but it had an impact on the dune retreat variability, especially for the most energetic event.

4.4 Implications for an EWS

Most of the EWSs (based on online and offline simulations) consider static pre-storm conditions. The present results suggest that the uncertainty associated with the pre-storm morphology is relevant for correctly identifying tipping point conditions such as berm depletion or dune dismantling. Even for moderate events (5- and 10-year events), the antecedent beach profile seems to be highly relevant to totally (or not) eroded the berm. This indicates that if the EWS focuses on coastal receptors such as recreational activities and beach user facilities located at the backshore (as found in many sites, e.g., Armaroli et al. [2013]), the risk uncertainties related to the selection of the pre-storm conditions are very high, implying possible large underestimations or overestimations of the risks. This is of particular relevance in this study area where beach cusps can induce a reasonable alongshore variability of the beach profile (partially corresponding to the high/low berm morphologies used in this study). On the other hand, if the receptors are located in the dune, the uncertainties caused by the initial beach morphology are lower (e.g., 2-4 m for the 25-year return period). However, the impact of the initial morphological conditions is also remarkable on dune retreat driven by more energetic events (i.e. 50-year return period), since the variability associated with this parameter can go from a 9 m-retreat to the total dune depletion (see Table 1), leading to dune breaching and the starting of overwash to the inner areas. Taking into account this variability can be highly relevant to define levels of protection and risk reduction actions.

While in theory, an online-based EWS would be more flexible to incorporate the variability of the antecedent beach morphology and thus reduce some uncertainties of its predictions, in the practice, data acquisition, processing, and implementation in the numerical model made this objective highly complicated. Conversely, the incorporation of such data in an offline-based EWS can be achieved by the simple addition of a new training dataset covering different beach

morphologies in a non-operational time window. This EWS can be used for a better risk prediction but also uncertainty analysis of a given event under different morphological conditions.

The uncertainty on the simulated berm and dune retreats related to storm duration is generally lower than that associated with the antecedent beach morphology for moderate events. Only when storm severity largely increased, storm duration is relevant and even determined the occurrence of dune breaching. This would indicate that in an EWS based on offline simulations, the variable storm duration might not be essential to condition the prediction system and still obtain accurate beach erosion predictions for moderate events, but modelers should be aware of the limitations for very energetic events. This way the training dataset supporting the offline-based simulations EWS can be highly reduced. However, it is important to remark that when creating the synthetic storms, the copula method or other statistical techniques must be employed to take into account the dependence between the random variables describing the storm and their natural variability.

5 Conclusions

Multiple one-dimensional XBeach simulations were performed to improve the understanding of the beach/dune system response to storm events with varying severity and duration, and antecedent beach morphologies, and ultimately to obtain more reliable operational coastal hazards prediction systems. The severity of the storm was defined based on different return periods (<1, 5, 10, 25, and 50 years) and the duration was established based on a linear adjustment with the Hs (derived from field data) and the upper and lower confidence levels. The beach morphologies implemented in the model covered the natural variability of this demonstration site reported by previous studies, with varying berm characteristics (height and width), and consequently subaerial beach volume, and submerged profile. Three morphological indicators were used: remaining berm width, dune retreat, and eroded volume. Regarding the impact of the pre-storm beach morphology variability in those indicators, it was observed that: i) initial beach conditions highly determined the post-storm berm width for the 5- and 10-year events; ii) antecedent morphology played a significant role in dune retreat mainly for the most severe event (50-year events); iii) the eroded volume highly depended on the pre-storm morphological conditions, but the percentage of the eroded volume relative to the initial conditions was very similar across those profile morphologies (except when dune dismantling was noticed), and; iv) the emerged morphology (LBT and LTT) did not remarkably impact any of these indicators. Regarding the storm duration effect, the results revealed that: i) when estimating the remaining berm width, this variable was only relevant for moderate events (5-year event); ii) storm duration mainly had importance in dune retreat on the 50-year event, in which it governed the occurrence of dune breaching, and; iii) the eroded volume response to changes in storm duration was similar regardless of the storm intensity, except for the 50-year event. These findings highlight that the pre-storm beach morphology and storm duration are very relevant aspects in determining the response of the coastal systems, and consequently, they should be included in EWSs devoted to coastal hazards. Also, the characteristics (location) of the coastal receptors increase the level of uncertainty of these variables.

While these findings are primarily applicable to similar sites to the demonstration site, the methodology developed here can be used as a benchmark test to assess and quantify the impact

of these variables in other coastal erosion prediction systems worldwide. Therefore, this study will help to reduce uncertainties and provide solid and scientific-based knowledge that can be useful for the implementation of more reliable coastal erosion EWSs (on- and offline-based simulations) and subsequent risk reduction measures.

Acknowledgments, Samples, and Data

This work is supported by the EW-COAST project with reference ALG-LISBOA-01-145-FEDER-028657 and attributed by the Foundation for Science and Technology, IP, supported by the Regional Operational Program of Algarve and the Regional Operational Program of Lisbon in its component FEDER and the Foundation for Science and Technology in its OE component. The authors would like to acknowledge the financial support of the Portuguese Foundation of Science and Technology (FCT) to CIMA through UIDP/00350/2020. The authors would like also to acknowledge Professor Joaquim Luis for his active participation in processing and sharing bathymetric information (http://w3.ualg.pt/~jluis/mirone/main.html) and to Luísa Bon de Sousa for topographic data acquisition and processing. We also acknowledge the Instituto Hidrográfico and Puertos del Estado who supplied wave and water level data. COSMO Program (Programa de Monitorização da Faixa Costeira de Portugal Continental) of Agência Portuguesa do Ambiente, co-funded by the Programa Operacional Sustentabilidade e Eficiência no Uso de Recursos (POSEUR), is also acknowledged for data availability (https://cosmo.apambiente.pt). Theocharis Plomaritis has been also co-financed by the 2014-2020 ERDF Operational Programme and by the Department of Economy, Knowledge, Business and University of the Regional Government of Andalusia. Project reference: FEDER-UCA18-107062 and the Spanish national funded project CRISIS, Project reference: PID2019-109143RB-I00. No financial conflicts of interest for any author. Data that supports the Summary Results, Tables and Figures of this study can be accessible upon an email request.

Appendix

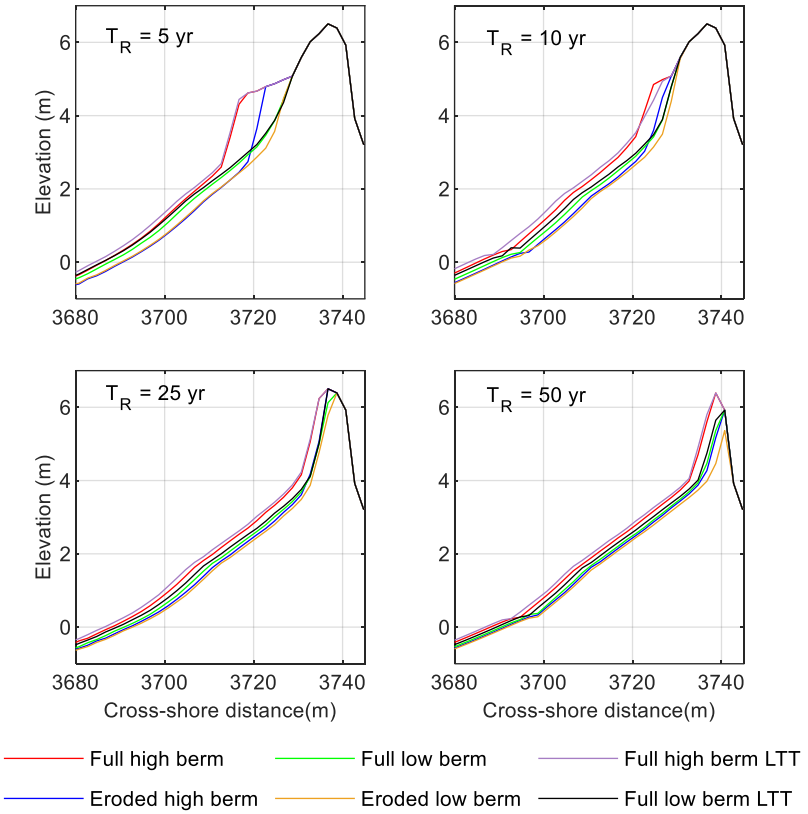

Figure A1. Simulated post-storm profiles for the events with duration 2.

References

Almeida, L. P., Ferreira, Ó., & Taborda, R. (2011a). Geoprocessing tool to model beach erosion due to storms: Application to Faro beach (Portugal). *Journal of Coastal Research*, (SPEC. ISSUE 64), 1830–1834.

Almeida, L. P., Ferreira, Ó., & Pacheco, A. (2011b). Thresholds for morphological changes on an exposed sandy beach as a function of wave height. *Earth Surface Processes and Landforms*, *36*(4), 523–532. https://doi.org/10.1002/esp.2072

Almeida, L. P., Vousdoukas, M. V., Ferreira, Ó., Rodrigues, B. A., & Matias, A. (2012). Thresholds for storm impacts on an exposed sandy coastal area in southern Portugal. *Geomorphology*, *143–144*, 3–12. https://doi.org/10.1016/j.geomorph.2011.04.047

Almeida, L. P. (2007). *Variabilidade do Perfil de Praia em Função da Agitação Marítima. Projecto Técnico-científico da Licenciatura em Oceanografia. Universidade do Algarve, Faculdade de Ciências e do Ambiente, Faro*.

Amores, A., Marcos, M., Carrió, Di. S., & Gomez-Pujol, L. (2020). Coastal impacts of Storm Gloria (January 2020) over the north-western Mediterranean. *Natural Hazards and Earth System Sciences*, *20*(7), 1955–1968. https://doi.org/10.5194/nhess-20-1955-2020

Anfuso, G., & Ruiz, N. (2004). Morfodinámica de una playa mesomareal expuesta con terraza de bejamar (Faro, Sur de Portugal). *Ciencias Marinas*, *30*(4), 575–584. https://doi.org/10.7773/cm.v30i4.341

Armaroli, C., Grottoli, E., Harley, M. D., & Ciavola, P. (2013). Beach morphodynamics and types of foredune erosion generated by storms along the Emilia-Romagna coastline, Italy. *Geomorphology*, *199*, 22–35. https://doi.org/10.1016/j.geomorph.2013.04.034

Arnoux, F., Abadie, S., Bertin, X., & Kojadinovic, I. (2021). Coastal flooding event definition based on damages: Case study of Biarritz Grande Plage on the French Basque coast. *Coastal Engineering*, 135907. https://doi.org/10.1016/j.coastaleng.2021.103873

Baldock, T. E., Gravois, U., Callaghan, D. P., Davies, G., & Nichol, S. (2021). Methodology for estimating return intervals for storm demand and dune recession by clustered and non-clustered morphological events. *Coastal Engineering*, *168*(August 2020), 103924. https://doi.org/10.1016/j.coastaleng.2021.103924

Balouin, Y., Howa, H., & Rafecas, N. (2000). Morphodynamique de croissants de plage, Plage de Faro, Sud Portugal. In *7th Colloque de l'Union des Océanographes Français, La Rochelle, France, June 2000* (p. 2000).

Barnard, P. L., van Ormondt, M., Erikson, L. H., Eshleman, J., Hapke, C., Ruggiero, P., et al. (2014). Development of the Coastal Storm Modeling System (CoSMoS) for predicting the impact of storms on high-energy, active-margin coasts. *Natural Hazards*, *74*(2), 1095–1125. https://doi.org/10.1007/s11069-014-1236-y

van Bemmelen, C. W. T., de Schipper, M. A., Darnall, J., & Aarninkhof, S. G. J. (2020). Beach scarp dynamics at nourished beaches. *Coastal Engineering*, *160*(July 2019), 103725. https://doi.org/10.1016/j.coastaleng.2020.103725

Beuzen, T., Harley, M. D., Splinter, K. D., & Turner, I. L. (2019). Controls of Variability in Berm and Dune Storm Erosion. *Journal of Geophysical Research: Earth Surface*, *124*(11), 2647–2665. https://doi.org/10.1029/2019JF005184

Booij, N., Ris, R. C., & Holthuijsen, L. H. (1999). A third-generation wave model for coastal regions: 1. Model description and validation. *Journal of Geophysical Research: Oceans*, *104*(C4), 7649–7666. https://doi.org/10.1029/98JC02622

Callaghan, D. P., Nielsen, P., Short, A., & Ranasinghe, R. (2008). Statistical simulation of wave climate and extreme beach erosion. *Coastal Engineering*, *55*(5), 375–390. https://doi.org/10.1016/j.coastaleng.2007.12.003

Callaghan, D. P., Ranasinghe, R., & Roelvink, D. (2013). Probabilistic estimation of storm erosion using analytical, semi-empirical, and process based storm erosion models. *Coastal*

Engineering, *82*, 64–75. https://doi.org/10.1016/j.coastaleng.2013.08.007

Castelle, B., Marieu, V., Bujan, S., Splinter, K. D., Robinet, A., Sénéchal, N., & Ferreira, S. (2015). Impact of the winter 2013-2014 series of severe Western Europe storms on a double-barred sandy coast: Beach and dune erosion and megacusp embayments. *Geomorphology*, *238*, 135–148. https://doi.org/10.1016/j.geomorph.2015.03.006

Cho, M., Yoon, H.-D., Yang, J.-A., & Son, S. (2019). Sensitivity and uncertainty analysis of coastal numerical model under various beach conditions in Korea. In *Proceedings of the 9th International Conference, Coastal Sediment 2019* (pp. 481–487).

Ciavola, P., Taborda, R., Ferreira, Ó., & Dias, J. A. (1997). Field observations of sand-mixing depths on steep beaches. *Marine Geology*, *141*(1–4), 147–156. https://doi.org/10.1016/S0025-3227(97)00054-6

Ciavola, P., Ferreira, O., Van Dongeren, A., Van Thiel de Vries, J., Armaroli, C., & Harley, M. (2014). Prediction of Storm Impacts on Beach and Dune Systems. *Hydrometeorological Hazards: Interfacing Science and Policy*, *9781118629*, 227–252. https://doi.org/10.1002/9781118629567.ch3d

Cohn, N., Ruggiero, P., García-Medina, G., Anderson, D., Serafin, K. A., & Biel, R. (2019). Environmental and morphologic controls on wave-induced dune response. *Geomorphology*, *329*, 108–128. https://doi.org/10.1016/j.geomorph.2018.12.023

Costa, M., Silva, R., & Vitorino, J. (2001). Contribuição para o Estudo do Clima de Agitação Marítima na Costa Portuguesa. In *II Jornadas Portuguesas de Engenharia Costeira e Portuária, Sines, Portuga*.

Crapoulet, A., Héquette, A., Marin, D., Levoy, F., & Patrice, B. (2017). Variations in the response of the dune coast of northern France to major storms as a function of available beach sediment volume. *Earth Surface Processes and Landforms*, *27*(January), 1603–1622. https://doi.org/10.1002/esp.4098

Van Dongeren, A., Ciavola, P., Viavattene, C., De Kleermaeker, S., Martinez, G., Ferreira, O., et al. (2014). RISC-KIT: Resilience-Increasing Strategies for Coasts - ToolKIT. *Journal of Coastal Research*, *70*, 366–371. https://doi.org/10.2112/SI70-062.1

Duo, E., Sanuy, M., Jiménez, J. A., & Ciavola, P. (2020). How good are symmetric triangular synthetic storms to represent real events for coastal hazard modelling. *Coastal Engineering*, *159*(August 2019). https://doi.org/10.1016/j.coastaleng.2020.103728

Eichentopf, S., Karunarathna, H., & Alsina, J. M. (2019). Morphodynamics of sandy beaches under the influence of storm sequences: Current research status and future needs. *Water Science and Engineering*, *12*(3), 221–234. https://doi.org/10.1016/j.wse.2019.09.007

Fairley, I., Horrillo-Caraballo, J., Masters, I., Karunarathna, H., & Reeve, D. E. (2020). Spatial Variation in Coastal Dune Evolution in a High Tidal Range Environment. *Remote Sensing*, *20*, 3689. https://doi.org/10.3390/rs12223689

Ferreira, Ó., Viavattene, C., Jim, J. A., Bolle, A., Neves, L., Plomaritis, T. A., et al. (2018). Storm-induced risk assessment : Evaluation of two tools at the regional and hotspot scale, *134*(September 2017), 241–253. https://doi.org/10.1016/j.coastaleng.2017.10.005

Ferreira, Ó., Martins, J. T., & Dias, J. A. (1997). Morfodinâmica e vulnerabilidade da Praia de Faro. *Livro de Comunicações Do Seminário Sobre a Zona Costeira Do Algarve, EUROCOAST Portugal*, 67–76.

Ferreira, Ó. (2005). Storm groups versus extreme single storms: predicted erosion and management consequences. *Journal of Coastal Research, SI*(42), 221–227.

Ferreira, Ó., Taborda, R., & Dias, J. A. (1998). Morphological Vulnerability Index: A Simple Way of Determining Beach Behaviour. In *Coastal Engineering* (pp. 3206–3214). https://doi.org/10.1061/9780784404119.243

Ferreira, Ó., Garcia, T., Matias, A., Taborda, R., & Dias, J. A. (2006). An integrated method for the determination of set-back lines for coastal erosion hazards on sandy shores. *Continental Shelf Research*, *26*(9), 1030–1044. https://doi.org/10.1016/j.csr.2005.12.016

Ferreira, Ó., Matias, A., & Pacheco, A. (2016). The East Coast of Algarve: a Barrier Island Dominated Coast. *Thalassas: An International Journal of Marine Sciences*, *32*(2), 75–85. https://doi.org/10.1007/s41208-016-0010-1

Ferreira, Ó., Plomaritis, T. A., & Costas, S. (2019). Effectiveness assessment of risk reduction measures at coastal areas using a decision support system: Findings from Emma storm. *Science of the Total Environment*, *657*, 124–135. https://doi.org/10.1016/j.scitotenv.2018.11.478

Fortunato, A. B., Li, K., Bertin, X., Rodrigues, M., & Miguez, B. M. (2016). Determination of extreme sea levels along the Iberian Atlantic coast. *Ocean Engineering*, *111*, 471–482. https://doi.org/10.1016/j.oceaneng.2015.11.031

Garzon, J., Ferreira, A., Ferreira, Ó., Fortes, C., & Reis, M. (2020). *Beach State Report: Quarteira, Praia de Faro and Costa da Caparica*. Retrieved from https://www.cima.ualg.pt/ew-coast/wp-content/uploads/2020/09/Beach_state_report-.pdf

Garzon, J. L., Costas, S., & Ferreira, Ó. (2021a). Biotic and abiotic factors governing dune response to storm events (under review). *Earth Surface Processes and Landforms*, *(Special Issue: Coastal dunes)*, submitted.

Garzon, J. L., Ferreira, Ó., & Plomaritis, T. A. (2021b). XBeach modeling of storm-driven erosion in natural and protected steep beaches. *Coastal Engineering Journal*, submitted.

Gravois, U., Baldock, T. E., Hsieh, S., Gomez, C., & Callaghan, D. P. (2016). Physical modelling of the effect of storm sequences on beach profile evolution and beach erosion. *NSW Coastal Conference*, 1–13.

Guisado-Pintado, E., & Jackson, D. W. T. (2018). Multi-scale variability of storm Ophelia 2017:

The importance of synchronised environmental variables in coastal impact. *Science of the Total Environment*, *630*, 287–301. https://doi.org/10.1016/j.scitotenv.2018.02.188

Haerens, P. (2009). *Seasonal and storm induced morphological variations at Praia de Faro, Península do Ancão, Southern Portugal.*

Harley, M. D., Valentini, A., Armaroli, C., Perini, L., Calabrese, L., & Ciavola, P. (2016a). Can an early-warning system help minimize the impacts of coastal storms? A case study of the 2012 Halloween storm, northern Italy. *Natural Hazards and Earth System Sciences*, *16*(1), 209–222. https://doi.org/10.5194/nhess-16-209-2016

Harley, M. D., Turner, I. L., Splinter, K. D., Phillips, M. S., & Simmons, J. A. (2016b). Beach response to Australian east coast lows: A comparison between the 2007 and 2015 events, Narrabeen-Collaroy Beach. *Journal of Coastal Research*, *1*(75), 388–392. https://doi.org/10.2112/SI75-078.1

Harley, M. D., Turner, I. L., Kinsela, M. A., Middleton, J. H., Mumford, P. J., Splinter, K. D., et al. (2017). Extreme coastal erosion enhanced by anomalous extratropical storm wave direction. *Scientific Reports*, *7*(1), 1–9. https://doi.org/10.1038/s41598-017-05792-1

Kriebel, D. L., & Dean, R. G. (1993). Convolution Method for Time-Dependent Beach-Profile Response. *Journal of Waterway, Port, Coastal and Ocean Engineering, ASCE*, *119*(2), 204–226. https://doi.org/https://doi.org/10.1061/(asce)0733-950x(1993)119:2(204)

Lavell, A., Oppenheimer, M., Diop, C., Hess, J., Lempert, R., Li, J., et al. (2012). *Climate change: New dimensions in disaster risk, exposure, vulnerability, and resilience*. *Managing the Risks of Extreme Events and Disasters to Advance Climate Change Adaptation: Special Report of the Intergovernmental Panel on Climate Change* (Vol. 9781107025). https://doi.org/10.1017/CBO9781139177245.004

Lerma, A. N., Bulteau, T., Muller, H., Decarsin, C., Gillet, R., Paris, F., et al. (2018). Towards the Development of a Storm Erosion EWS for the French Aquitaine Coast. *Journal of Coastal Research*, *85*(May), 666–670. https://doi.org/10.2112/SI85-134.1

Luijendijk, A., Hagenaars, G., Ranasinghe, R., Baart, F., Donchyts, G., & Aarninkhof, S. (2018). The State of the World's Beaches. *Scientific Reports*, *8*(1), 1–11. https://doi.org/10.1038/s41598-018-24630-6

Malvarez, G., Ferreira, Ó., Navas, F., Cooper, J. A. G., Gracia-Prieto, F. J., & Talavera, L. (2021). Storm impacts on a coupled human-natural coastal system : Resilience of developed coasts. *Science of the Total Environment*, *768*, 144987. https://doi.org/10.1016/j.scitotenv.2021.144987

Martins, J. T., Ferreira, Ó., & Dias, J. A. (1997). A susceptibilidade da Praia de Faro à erosão por tempestades. *9º Congresso Do Algarve*, 206–213.

Martins, J. T., Ferreira, Ó., Ciavola, P., & Dias, J. A. (1996). Monitoring of Profile Changes at Praia de Faro (Algarve): a Tool to Predict and Solve Problems. *Partnership in Coastal Zone*

Management, Samara Publishing, 615–622.

Masselink, G., & Short, A. D. (1993). *The Effect of Tide Range on Beach Morphodynamics and Morphology: A Conceptual Beach Model*. *Journal of Coastal Research*.

Mendoza, E. T., Jimenez, J. A., & Mateo, J. (2011). A coastal storms intensity scale for the Catalan sea (NW Mediterranean). *Natural Hazards and Earth System Science*, *11*(9), 2453–2462. https://doi.org/10.5194/nhess-11-2453-2011

Mentaschi, L., Vousdoukas, M. I., Pekel, J. F., Voukouvalas, E., & Feyen, L. (2018). Global long-term observations of coastal erosion and accretion. *Scientific Reports*, *8*(1), 1–11. https://doi.org/10.1038/s41598-018-30904-w

Pires, H. O. (1998). Project INDIA. Preliminary report on wave climate at Faro. Instituto de Meteorologia, IST, Lisboa, Portugal.

Plomaritis, T. A., Ferreira, Ó., Costas, S., & Puig, M. (2019). Storm induced coastal erosion: indicators selection and comparison of three modelling approaches. In *X Jornadas de Geomorfología Litoral* (pp. 37–40).

Plomaritis, T. A., Costas, S., & Ferreira, O. (2018). Use of a Bayesian Network for coastal hazards, impact and disaster risk. *Coastal Engineering*, *134*(February 2017), 134–147. https://doi.org/10.1016/j.coastaleng.2017.07.003

Poelhekke, L., Jäger, W. S., van Dongeren, A., Plomaritis, T. A., McCall, R., & Ferreira, Ó. (2016). Predicting coastal hazards for sandy coasts with a Bayesian Network. *Coastal Engineering*, *118*, 21–34. https://doi.org/10.1016/j.coastaleng.2016.08.011

Ranasinghe, R. (2016). Assessing climate change impacts on open sandy coasts: A review. *Earth-Science Reviews*, *160*, 320–332. https://doi.org/10.1016/j.earscirev.2016.07.011

Rodrigues, B. A., Matias, A., & Ferreira, Ó. (2012). Overwash hazard assessment. *Geologica Acta*, *10*(4), 427–437. https://doi.org/10.1344/105.000001743

Roelvink, D., Reniers, A., van Dongeren, A., van Thiel de Vries, J., McCall, R., & Lescinski, J. (2009). Modelling storm impacts on beaches, dunes and barrier islands. *Coastal Engineering*, *56*(11–12), 1133–1152. https://doi.org/10.1016/j.coastaleng.2009.08.006

Roelvink, D., Mccall, R., Costas, S., & van der Lugt, M. A. (2019). Controlling swash zone slope is key to beach profile modelling. In *Proceedings of the 9th International Conference, Coastal Sediment 2019* (p. 149,157).

Sá-Pires, A. C., Taborda, R., Ferreira, Ó., Dias, J. A., & Grande, C. (2006). Beach Volume Changes : Vertical Datum Definition. *Journal of Coastal Research*, (SI 39), 341–344.

Sallenger, A. H. (2000). Storm Impact Scale for Barrier Islands. *Journal of Coastal Research*, *16*(3), 890–895.

Sánchez-Arcilla, A., Mendoza, E. T., Jiménez, J. A., Peña, C., Galofré, J., & Novoa, M. (2009). Beach Erosion and Storm Parameters: Uncertainties for the Spanish Mediterranean, (May), 2352–2362. https://doi.org/10.1142/9789814277426_0194

Santos, V. M., Wahl, T., Long, J. W., Passeri, D. L., & Plant, N. G. (2019). Combining Numerical and Statistical Models to Predict Storm-Induced Dune Erosion. *Journal of Geophysical Research: Earth Surface*, 1817–1834. https://doi.org/10.1029/2019JF005016

Sanuy, M., Duo, E., Jäger, W. S., Ciavola, P., & Jiménez, J. A. (2018). Linking source with consequences of coastal storm impacts for climate change and risk reduction scenarios for Mediterranean sandy beaches. *Natural Hazards and Earth System Sciences*, *18*(7), 1825–1847. https://doi.org/10.5194/nhess-18-1825-2018

Scott, T., Masselink, G., O'Hare, T., Saulter, A., Poate, T., Russell, P., et al. (2016). The extreme 2013/2014 winter storms: Beach recovery along the southwest coast of England. *Marine Geology*, *382*, 224–241. https://doi.org/10.1016/j.margeo.2016.10.011

Seok, J. S., & Suh, S. W. (2018). Efficient Real-time Erosion Early Warning System and Artificial Sand Dune Breaching on Haeundae Beach, Korea. *Journal of Coastal Research*, *85*, 186–190. https://doi.org/10.2112/SI85-038.1

Simmons, J. A., Splinter, K. D., Harley, M. D., & Turner, I. L. (2019). Calibration data requirements for modelling subaerial beach storm erosion. *Coastal Engineering*, *152*(November 2018), 103507. https://doi.org/10.1016/j.coastaleng.2019.103507

Smallegan, S. M., Irish, J. L., Van Dongeren, A. R., & Den Bieman, J. P. (2016). Morphological response of a sandy barrier island with a buried seawall during Hurricane Sandy. *Coastal Engineering*, *110*, 102–110. https://doi.org/10.1016/j.coastaleng.2016.01.005

Splinter, K. D., Carley, J. T., Golshani, A., & Tomlinson, R. (2014). A relationship to describe the cumulative impact of storm clusters on beach erosion. *Coastal Engineering*, *83*, 49–55. https://doi.org/10.1016/j.coastaleng.2013.10.001

Splinter, K. D., Kearney, E. T., & Turner, I. L. (2018). Drivers of alongshore variable dune erosion during a storm event: Observations and modelling. *Coastal Engineering*, *131*, 31–41. https://doi.org/10.1016/j.coastaleng.2017.10.011

Stockdon, H. F., Holman, R. A., Howd, P. A., & Sallenger, A. H. (2006). Empirical parameterization of setup, swash, and runup. *Coastal Engineering*, *53*(7), 573–588. https://doi.org/10.1016/j.coastaleng.2005.12.005

Valchev, N., Andreeva, N., Eftimova, P., & Trifonova, E. (2014). Prototype of early warning system for coastal storm hazard (Bulgarian black sea \coast). *Comptes Rendus de L'Academie Bulgare Des Sciences*, *67*(7), 971–978.

Valchev, N., Eftimova, P., & Andreeva, N. (2016). Implementation and validation of a multi-domain coastal hazard forecasting system in an open bay. *Coastal Engineering*, (this issue), 1–17. https://doi.org/10.1016/j.coastaleng.2017.08.008

Vousdoukas, M. I., Almeida, L. P. M., & Ferreira, Ó. (2012a). Beach erosion and recovery during consecutive storms at a steep-sloping, meso-tidal beach. *Earth Surface Processes and Landforms*, *37*(6), 583–593. https://doi.org/10.1002/esp.2264

Vousdoukas, M. I., Ferreira, Ó., Almeida, L. P., & Pacheco, A. (2012b). Toward reliable storm-hazard forecasts: XBeach calibration and its potential application in an operational early-warning system. *Ocean Dynamics*, *62*(7), 1001–1015. https://doi.org/10.1007/s10236-012-0544-6

Vousdoukas, M. I., Ranasinghe, R., Mentaschi, L., Plomaritis, T. A., Athanasiou, P., Luijendijk, A., & Feyen, L. (2020). Sandy coastlines under threat of erosion. *Nature Climate Change*, *in press*. https://doi.org/10.1038/s41558-020-0697-0